Life Sciences, Vol. 46, pp. 105-119 Pergamon Press
Printed in the U.S.A.

STEADY-STATE THEORY FOR QUANTITATIVE MICRODIALYSIS OF SOLUTES AND WATER *IN VIVO* AND *IN VITRO*

Peter M. Bungay, Paul F. Morrison, Robert L. Dedrick

Biomedical Engineering & Instrumentation Branch, Division of Research Services, National Institutes of Health, Bethesda, MD 20892 USA

(Received in final form November 9, 1989)

Summary

A mathematical framework was developed to provide a quantitative basis for either *in vivo* tissue or *in vitro* microdialysis. Established physiological and mass transport principles were employed to obtain explicit expressions relating dialysate concentration to tissue extracellular concentration for *in vivo* applications or external medium concentrations for *in vitro* probe characterization. Some of the important generalizations derived from the modeling framework are: (i) the microdialysis probe can perturb the spatial concentration profile of the substance of interest for a considerable distance from the probe, (ii) for low molecular weight species the tissue is generally more important than the probe membrane in determining the dialysate-to-tissue concentration relationship, (iii) metabolism, intracellular-extracellular and extracellular-microvascular exchange, together with diffusion, determine the role of the tissue in *in vivo* probe behavior, and, consequently, (iv) *in vitro* "calibration" procedures could be useful for characterizing the probe, if properly controlled, but have limited applicability to *in vivo* performance. The validity of the proposed quantitative approach is illustrated by the good agreement obtained between the predictions of a model developed for tritiated water ($[^3]H_2O$) in the brain and experimental data taken from the literature for measurements in the caudoputamen of rats. The importance of metabolism and efflux to the microvasculature is illustrated by the wide variation in predicted tissue concentration profiles among $[^3]H_2O$, sucrose and dihydroxyphenylacetic acid (DOPAC).

According to a recent bibliography (1) and a review (2), the use of dialysis for sampling extracellular tissue concentrations was demonstrated by 1972 (3), following initial reports appearing as early as 1966 (4). However, to date, use of the technology has been primarily empirical in the absence of a quantitative theory. "Calibration" conditions *In vitro* have typically been ill-defined, and equivocal interpretations have been applied to *in vivo* measurements.

This report describes a recently suggested general theoretical framework for microdialysis (5). The framework utilizes the mass transfer resistance concept underlying the approach adopted by Jacobson et al. (6). In contrast to these authors, who treated the overall probe-external medium mass transfer coefficient as an unknown fitting parameter, we show that this mass transfer coefficient can be predicted from

0024-3205/90 $3.00 + .00

knowledge of the relevant physical, physiological and biochemical processes. The analysis of Benveniste and co-workers (2,7) focuses on differences (*in vivo* versus *in vitro*) in path length and volume fraction accessible for diffusion through the medium surrounding the probe. We propose that *in vivo* analysis must consider metabolism and exchange between tissue and blood, in general, as well as the diffusional aspects. We show ways in which these processes can be included. For simplicity, the theory is presented in the context of a probe operating at steady-state. Extension of the concepts to transient operating conditions will be treated in subsequent reports.

In addition to the general framework, we develop a specific mathematical model for sampling tritiated water from the brain as a quasi-steady-state example and show the utility of the model in interpreting data from the literature. Predictions for hydrophilic solutes are summarized as well.

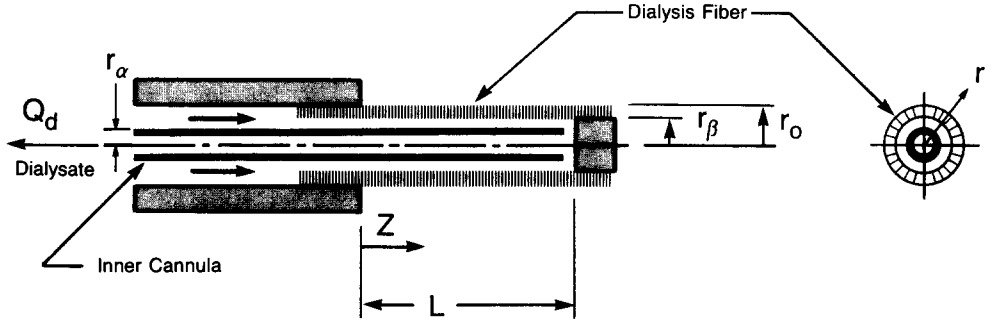

FIG. 1

Schematic views of microdialysis probe showing cylindrical coordinates (r, z) used in theoretical analysis. Dialysate solution flows at a constant volumetric rate, Q_d, through the annular space between the membrane and the inner cannula and through the cannula lumen. The assumed direction of flow is arbitrary. The radii of the outer cannula surface, inner membrane surface and outer membrane surface are denoted by r_α, r_β and r_o, respectively, and the length of dialysis membrane accessible for exchange between dialysate and external medium by L.

Steady-State Framework

The assumed probe configuration is shown schematically in Figure 1. The probe membrane is a cylindrical hollow fiber. The membrane hydraulic conductivity and transmembrane pressure differences, both hydrostatically and osmotically derived, are assumed to be sufficiently small that no appreciable transmembrane fluid flow is produced. Hydraulic conductivity values for some common dialysis hollow fiber membranes have been published (8).

Many of the hollow fibers membranes used in microdialysis probes were developed for hemodialysis. The hemodialysis literature has long employed the mass transfer resistance concept as a convenient tool for characterizing hemodialyzer performance. The concept is equally useful for describing mass flow through a microdialysis probe and its surroundings. A mass transport resistance (R) expresses the proportionality between a concentration driving force and the resultant mass flow. If ΔC is the radial

concentration difference across a given annular structure, e.g., the probe membrane, and q is the resulting mass flow rate across the structure in the radial direction, then the corresponding R for a differential length, dz, can be defined by

$$R = \frac{\Delta C}{q}. \qquad (1)$$

Eq.(1) is analogous to Ohm's Law ($R=\Delta V/I$) in which electrical resistance is the proportionality coefficient between an electrical potential difference (ΔV) and the resultant electrical current (I). The quantities q and ΔC vary with axial position, z. In general, R also varies with z. To simplify this presentation, R is taken to be the axial average value. A further implicit assumption is that the structures are symmetric about the probe axis or that the value of R is the average over all azimuthal angles.

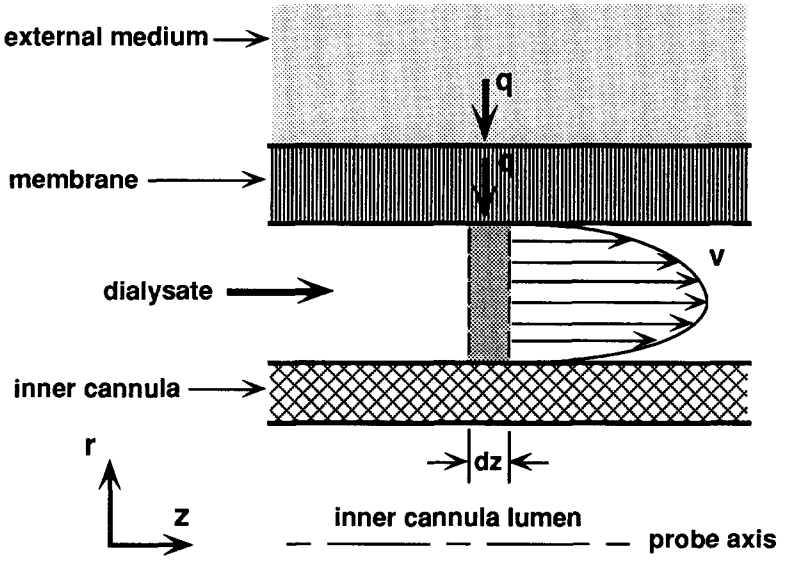

FIG. 2

Dialysate volume (gray, bounded by dashed lines) of differential axial thickness, dz, used in the derivation of mass balance Eq.(3). Dialysate enters and leaves the volume at a velocity, v, which varies in the radial (r) direction. A mass flow, q, enters the volume by diffusion from the adjacent membrane causing the flow-averaged dialysate concentration to increase by the differential amount, $d\bar{C}_d$.

The resistances for the dialysate (d), membrane (m) and external medium (ext) are additive, since they are in series and the mass flow, q, is the same across the dialysate-membrane and membrane-external medium interfaces as shown in Figure 2. Combining the defining equations for the three resistances gives

$$C_e^{\infty} - \bar{C}_d[z] = (R_d + R_m + R_{ext})q\,, \qquad (2)$$

in which C_e^{∞} is the uniform freely diffusible species concentration far enough from the

probe to be undisturbed by the probe presence. The overbar denotes that the dialysate concentration at location z, $C_d[z]$, has been averaged over the annulus cross-section in a manner that takes into account the radial variation in dialysate velocity indicated in Figure 2. The definition for this "flow-averaging" is given in the Nomenclature section. A steady-state mass balance over a dialysate volume of differential thickness, dz, defined in Figure 2 gives

$$q = Q_d L\left(\frac{d\bar{C}_d}{dz}\right). \tag{3}$$

Combining Eqs.(2) and (3) and integrating over the accessible length of the membrane from the inlet, z=0, to the outlet, z=L, leads to the desired relationship between C_e^∞ and the dialysate inlet and outlet concentrations, $C_d^{in}=\bar{C}_d[0]$ and $C_d^{out}=\bar{C}_d[L]$. By analogy to the description of plasma-tissue exchange in the microvasculature (ref. 9 and Eq.(A6) of the Appendix) the relationship assumes the form of a "dialysate extraction fraction"

$$E_d = \frac{C_d^{out}-C_d^{in}}{C_e^\infty - C_d^{in}} = 1-\exp\left[-\frac{1}{Q_d(R_d+R_m+R_{ext})}\right]. \tag{4}$$

The analogy between Eq.(4) and Appendix Eq.(A6) is made clearer by defining an overall probe-external medium permeability (P) and surface area (S) product as

$$PS = \frac{1}{R_d+R_m+R_{ext}}. \tag{5}$$

The permeability, P, is equivalent to the mass transfer coefficient of Jacobson et al. (6).

In the remaining analysis explicit expressions are written for the probe resistances (R_d and R_m) and the external resistance when the probe is situated either in tissue ($R_{ext}=R_e$), a quiescent medium ($R_{ext}=R_q$), or a well-stirred solution ($R_{ext}=R_s$). Each resistance will be expressed in the general form

$$R = \frac{\Delta r}{D_{eff}S\phi}, \tag{6}$$

in which the length, Δr, the effective diffusion coefficient, D_{eff}, the surface area, S, and the medium volume fraction accessible to the diffusing species, ϕ, are different for each resistive medium. To obtain these expressions modeling assumptions concerning the behavior of the chemical species of interest will be invoked. The set of assumptions to be used provides a useful starting point for the quantitative description of microdialysis behavior. The substitution of a different set of assumptions may lead to altered expressions for the resistances, which nevertheless are likely to fit within the above general mass transport resistance framework.

Mass Transport Resistances

Dialysate: Let the characteristic length in Eq.(6) be the annulus thickness, $\Delta r_d=r_\beta-r_\alpha$, the characteristic area be that of the inner membrane surface, $S_d=2\pi r_\beta L$, and $\phi_d=1$. For laminar flow in the annular dialysate channel, $(D_{eff})_d=\vartheta D_d$, in which D_d is the diffusion coefficient in the dialysate. The coefficient ϑ is a function of the geometry of the channel and the ratio of the annulus residence time, $T_Q=\pi(r_\beta^2-r_\alpha^2)L/Q_d$, to a time, $T_D=(r_\beta-r_\alpha)^2/D_d$, characteristic of trans-annulus diffusion. The highest values for R_d correspond to

situations in which $T_D<T_Q$. We have used as an approximation the value $\vartheta=35/13$ for uniform mass flux into a thin annulus under conditions of $T_D<T_Q$ to obtain (based on a similar analysis in ref. 10)

$$R_d = \frac{13(r_\beta - r_\alpha)}{70\pi L r_\beta D_d}. \qquad (7)$$

Membrane: For low molecular weight water-soluble solutes the accessible volume fraction of the membrane, ϕ_m, is of the order of the volume fraction occupied by water. Diffusion of the compound within the accessible volume fraction is characterized by an effective diffusion coefficient, D_m, which can incorporate additional effects such as reversible binding, hindrance (11) and tortuosity. If only the latter two effects are significant, $D_m=D_dH_m/\lambda_m^2$, in which H_m is a fractional hindered diffusion factor and λ_m is a tortuosity factor. The membrane resistance,

$$R_m = \frac{\ell n(r_o/r_\beta)}{2\pi L D_m \phi_m}, \qquad (8)$$

is obtained by integrating Appendix Eq.(A3). Eqs.(6) and (8) lead to the definitions $\Delta r_m=r_o-r_\beta$, $(D_{eff})_m=D_m$, and $S_m=(S_o-S_\beta)/\ell n(S_o/S_\beta)$. The latter is the logarithmic mean of the membrane outer and inner surface areas, $S_o=2\pi r_o L$ and $S_\beta=2\pi r_\beta L$, respectively.

For a given probe (i.e., fixed r_β, r_o and L) the membrane resistance depends on $D_m\phi_m$. Some data are available in the literature for dialysis membrane permeabilities (P_m) to marker solutes, e.g., in references (8) and (11), from which $D_m\phi_m$ values can be calculated ($D_m\phi_m=P_m\Delta r_m$). From these values one can often estimate R_m given knowledge of key physical properties, such as molecular weight, shape and charge for the chemical species of interest.

Tissue ($R_{ext}=R_e$): For the probe inserted in tissue it is assumed that the surrounding tissue is in a normal state and is in intimate contact with the outer surface of the probe. Diffusible species can be considered to move along two parallel pathways through the tissue: extracellular and transcellular. It is possible to include both pathways in the theoretical description. However, for water-soluble solutes the difference in the resistance offered by the two pathways is such that, in general, the contribution of the transcellular pathway can be neglected (12). The additional assumption that the transport processes are linear in the chemical species concentration leads to Appendix Eqs.(A4)-(A10), from which the following tissue resistance expression can be obtained

$$R_e = \frac{(K_0/K_1)\Gamma}{2\pi r_o L D_e \phi_e}. \qquad (9)$$

In the above, K_0 and K_1 are modified Bessel functions of the second kind with dimensionless argument r_o/Γ. Values of the Bessel functions are tabulated in handbooks such as ref. (13). The concentration profile penetration depth parameter, Γ, is given by

$$\Gamma = \sqrt{\frac{D_e}{k_{ep}^x + k_e^r + k_c^r}}. \qquad (10)$$

The parameters summed within the parentheses in Eq.(10) are first order rate constants representing efflux to the microvasculature (k_{ep}^x), irreversible extracellular metabolism (k_e^r), and the effect of irreversible intracellular metabolism (k_i^r) and extracellular-

intracellular exchange (k_{ei}^x and k_{ie}^x) through the composite rate constant, k_c^r, which is given by Appendix Eq.(A10). The choice of $S_e=2\pi r_o L$ and $(D_{eff}\phi)_e$ as the product of the extracellular fluid (ECF) effective diffusion coefficient, D_e, and volume fraction, ϕ_e, leaves $\Delta r_e=(K_0/K_1)\Gamma$ in Eq.(6). The tortuosity (2,7,12,14) and hindered diffusion effects included in D_e can be represented by $D_e=D_d H_e/\lambda_e^2$, in which H_e is the fractional reduction in diffusion coefficient owing to hindered diffusion and λ_e is a relative measure of the increase in diffusional path length owing to tortuosity. This expression neglects other effects, such as reversible binding.

For a given probe (i.e., fixed r_β, r_o and L), the tissue resistance depends on k_{ep}^x, k_e^r, and k_c^r as well as $D_e\phi_e$. Thus, it is not possible to generalize for R_e, as it is for R_m, based on knowledge of only the species molecular weight, shape and charge. One also requires information on the efflux, metabolism and cell membrane transport processes in order to estimate R_e. It is of interest to note that rate constants for influx and generation do not appear in Eq.(10) and, hence, do not affect R_e or the relationship between the undisturbed extracellular concentration, C_e^∞, and the dialysate concentrations given by Eq.(4). According to Appendix Eq.(A8), influx and generation do, however, play a role in determining the level of C_e^∞.

Quiescent Medium ($R_{ext}=R_q$): As a reference against which to compare the tissue resistance, it is instructive to examine the external resistance for the probe placed in a quiescent dialysate solution ($D_{eff}\phi=D_d$) or inert medium (e.g., a gel) in which only diffusion occurs. An approximate expression for this situation, as derived in the Appendix, is

$$R_q = \frac{1}{2\pi D_q \phi_q \sqrt{2r_o L}}, \qquad (11)$$

for which $(D_{eff}\phi)_q=D_q\phi_q$, $S_q=2\pi r_o L$ and $\Delta r_q=\sqrt{(r_o L/2)}$ to satisfy Eq.(6).

Well-Stirred Medium ($R_{ext}=R_s$): The probe transport resistances, R_d and R_m, are perhaps best studied under conditions of vanishing external resistance. In a perfectly mixed external medium

$$R_s = 0 . \qquad (12)$$

Examples

In order to utilize the above theoretical framework for tissue studies, it is not sufficient to have information on the diffusion coefficients, D_d, D_m and D_e, the corresponding volume fractions, and the probe geometry. According to Eqs.(9-10) one also requires values for whichever exchange and metabolism rate constants are relevant for the chemical species of interest. Three species will be considered as illustrations. The estimates for the rate constants differ widely among the species chosen. Model predictions of two types will be examined: (i) the dialysate extraction fraction ("recovery") and its dependence on dialysate flow rate (Figure 3), and (ii) the differences among the chemical species extracellular concentration profiles in tissue (Figure 4).

Tritiated Water ($[^3]H_2O$): Tritiated water will be presented as a detailed illustrative example because the use of microdialysis for sampling $[^3]H_2O$ from rat brain *in vivo* has been documented in the literature (15). For $[^3]H_2O$ the metabolism rate constants, k_e^r and

k_i^r, can be neglected in comparison with the high value for the rate constant, k_{ep}^x, for efflux from ECF to plasma. Independent experimental measurements are available for the parameter, Γ, in dog caudate nucleus (12). Setting the diffusion coefficient, D_e, for $[3]H_2O$ in ECF equal to the value for diffusion in water (i.e., letting $H_e=\lambda_e=1$) leads to a value of $\phi_e=0.25$ for fitting Eq.(4) to the *in vivo* data (Figure 3). Reducing the D_e value to account for tortuosity ($\lambda_e>1$) and hindrance effects ($H_e<1$) would yield a higher value for ϕ_e. This suggests a contribution from transcellular, as well as extracellular, diffusion for $[3]H_2O$, since the ECF volume fraction obtained for exclusively extracellular solutes tends to be smaller (e.g., $\phi_e=0.175$ for sucrose from ref. 12).

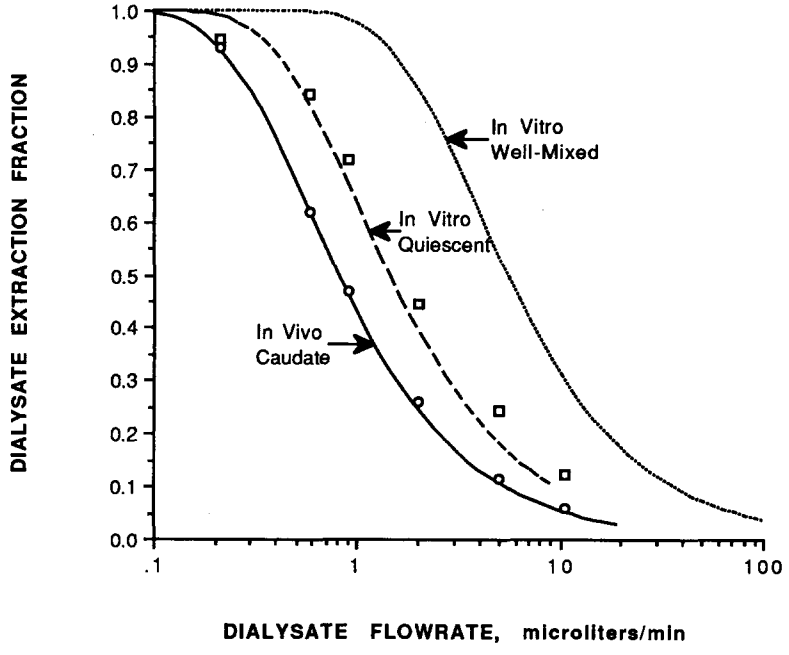

FIG. 3

Influence of dialysate flow rate (Q_d) on microdialysis extraction fraction (E_d) for sampling tritiated water with a probe whose accessible membrane length is L=3 mm. The curves are plots of theoretical predictions from Eqs.(4-12) based on D_d= 2.1 x10^{-5} cm^2/s at 22°C and D_d=3.0x10^{-5} cm^2/s at 37°C from measurements of $[3]H_2O$ diffusing in water (16). Three external media are simulated: (i) dog caudate, $\Gamma=\sqrt{D_e/k_{ep}^x}$=0.062 cm (12) and D_e=3.0x10^{-5} cm^2/s for ϕ_e=0.25 (solid curve), (ii) quiescent solution of $[3]H_2O$ at 22°C (dashed curve), and (iii) well-mixed solution of $[3]H_2O$ at 22°C (dotted curve). The points represent data from Alexander et al. (15) obtained in the absence of $[3]H_2O$ in the dialysate entering the probe (C_d^{in}=0, E_d="recovery"). Probes were placed either in the caudoputamen of Long-Evans hooded rats following an intravenously administered dose of $[3]H_2O$ (circles), or immersed in a $[3]H_2O$ solution at room temperature (20-23°C) (squares). The parameters used for the probes were estimated to be: r_α=0.125 mm, r_β=0.20 mm, r_o=0.25 mm, and $D_m\phi_m=0.3D_d$ (11).

Solutes: Two solutes to be considered briefly are sucrose and dihydroxyphenylacetic acid (DOPAC). Although the detailed models for these two species have not, as yet, been validated, they are based on available experimental evidence. The range of behavior predicted should be illustrative of that expected, in general, for low molecular weight, hydrophilic solutes. Figure 4 shows the steady-state concentration profiles that would be developed in the brain as the result of sampling these two solutes and $[^3]H_2O$ at a typical dialysate flow rate of 1μl/min. The concentrations in the dialysate annulus are indicative of the relative differences in E_d ("recovery") for these three species.

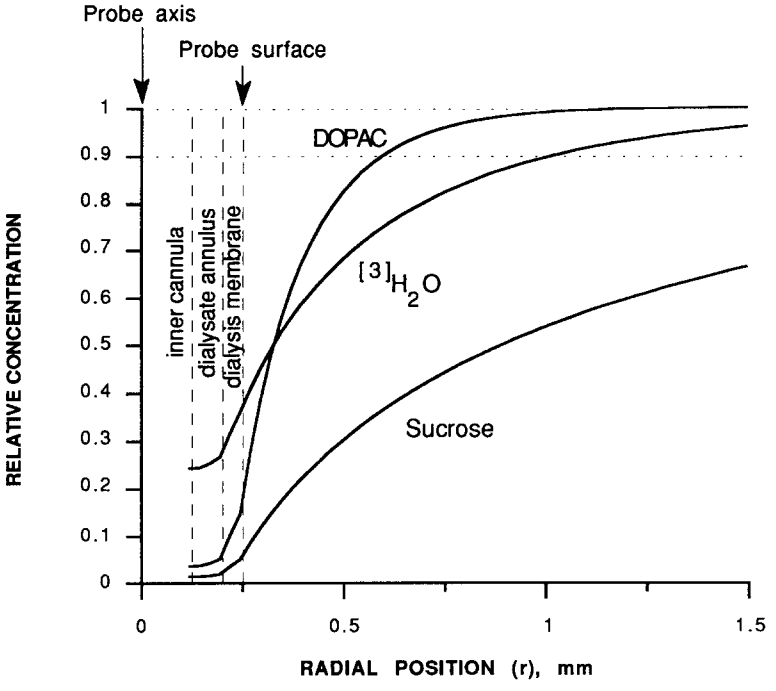

FIG. 4

Steady-state, spatial concentration profiles in brain on the probe midplane (z=L/2) in the direction perpendicular to the probe axis calculated from Appendix Eqs.(A11)-(A13) for dialysate flow rate Q_d = 1 μl/min. The ordinate is the ratio of the local concentration to the distant extracellular fluid concentration, C_e^∞. Probe membrane values, D_m and ϕ_m, were estimated from measurements and molecular weight correlations in ref.(11). For tritiated water ($[^3]H_2O$) (see Figure 3 caption): D_d=3.0x10^{-5} cm^2/s, $D_m\phi_m$=0.3D_d, $D_e\phi_e$=0.25D_d, k_{ep}^x=0.46 min^{-1} (12), k_e^r=k_e^c=0, and Γ=0.062 cm. For sucrose: D_d=7.0x10^{-6} cm^2/s and $D_m\phi_m$=0.2D_d (11), D_e=3.1x10^{-6} cm^2/s and ϕ_e=0.175 (12), k_{ep}^x=ps/ϕ_e=2.1x10^{-3} min^{-1} (9), k_e^r=k_e^c=0, and Γ=0.30 cm. For dihydroxyphenylacetic acid (DOPAC): D_d=7.4x10^{-6} cm^2/s (14), $D_m\phi_m$=0.2D_d (11), ϕ_e=0.175 (12), D_e=2.5x10^{-6} cm^2/s (14), $G_i\phi_i$=23 nmol/(cm^{3}hr) and C_i^∞=5.9 nmol/cm^3 (17) giving $k_{ep}^x+k_e^r+k_e^c$=0.37 min^{-1} and Γ=0.02 cm, assuming k_{ei}^x=k_{ie}^x=6 min^{-1}. The probe geometric parameters were estimated to be: r_α=0.125 mm, r_β=0.20 mm, and r_o=0.25 mm, with L chosen to be 3 mm.

Discussion

The present theoretical development can be used to describe microdialysis when the probe acts either as a sampling device or as a means for localized delivery of an agent from the dialysate to the surrounding medium. The discussion will focus on the former application. A number of general observations can be made based on the microdialysis predictions for $[^3]H_2O$ and several low molecular weight, water-soluble solutes (acetaminophen and cis-platin, in addition to sucrose and DOPAC). Several of the more important points are as follows.

For the compounds and probe membranes thus far examined $R_e >> R_m >> R_d$, that is, the tissue presents the dominant resistance. This corresponds to the feature illustrated in Figure 4 that the majority of the drop between the distant extracellular concentration (C_e^∞) and the dialysate concentration occurs within the tissue. When the tissue resistance is dominant, the choice of dialysis membrane material is relatively unimportant. The relative magnitude of R_e and R_m may be different for higher molecular weight solutes because of differences in the molecular weight dependence of the two media. For example, the common cellulosic hemodialysis membranes are poorly permeable to globular solutes above 10,000 daltons (8,11) in comparison to most tissue extracellular spaces. It is conceivable that one might choose a probe membrane so restrictive that $R_m >> R_e$ even for low molecular solutes in order to obtain similar extraction fractions *in vivo* and *in vitro.* However, one would expect that the dialysate extraction fraction, E_d, will be much lower than for the current probes. All three resistances are additive, and any increase in the total resistance causes E_d to decrease according to Eq.(4). In principle, assuming sufficiently sensitive techniques are available for assaying low dialysate concentrations, the use of a high resistance probe membrane could be an attractive approach to simplifying probe calibration.

When the R_e is dominant and E_d is low, the extracellular concentration can be disturbed for a considerable distance from the probe. This important point was demonstrated experimentally by Benveniste et al. (7), who determined that calcium ions in the brain were depleted over a distance of the order of 1 mm from the probe surface. It is further illustrated for three varied substances by theoretical predictions in Figure 4 produced by the current theory. The distance to which the concentration profile penetrates into the tissue varies with the chemical species and is determined, according to Appendix Eq.(A9), by the ratio Γ/r_o. Despite the relatively high E_d for the the flow rate selected, the presence of the probe depresses $[^3]H_2O$ concentration below 90% of the undisturbed value for a distance of about 1 mm from the probe axis (0.75 mm from the probe surface) because $\Gamma/r_o=2.5$. The ratio Γ/r_o decreases with decreasing diffusivity or increasing efflux and metabolism, according to Eq.(10). For the actively metabolized solute, DOPAC ($\Gamma/r_o=0.8$), the predicted 90% penetration distance is still 0.35 mm. On the other hand, the distance could be considerably larger for a species with $\Gamma/r_o >> 1$, such as a nonmetabolized solute of low microvascular permeability. For example, the predicted 90% penetration distance for sucrose ($\Gamma/r_o=12.0$) is greater than 3 mm! The predicted distance would be less if diffusion in the axial, as well as radial, direction were included in the model. Nevertheless, the distance would be a large fraction of the rat brain dimensions. The penetration distance is of importance when one attempts either to sample from a small structure or to stimulate a limited portion of a tissue with an agent being delivered in the dialysate.

The considerable variation in extracellular concentration displayed in Figure 4 could have significance for the transport characteristics of the affected tissue. If the

metabolism and exchange processes are linear in concentration as assumed, then the tissue resistance for the substance is unaffected by the spatial variation in its concentration. However, it should be remembered that the concentrations of all dialyzable substances can be altered in the vicinity of the probe, and among these may be modulators of processes involving the substance(s) of interest. One approach to checking on the assumptions of linearity and uniformity of R_e consists of perfusing the probe with solutions containing differing inlet concentrations of the substance being studied (18-19). If the assumptions are valid, a plot of $C_d^{out}-C_d^{in}$ against C_d^{in} should yield a straight line of slope $-[1-\exp(-PS/Q_d)]$ and intercept C_e^{∞} on the abscissa, according to Eq.(4). Lönnroth et al. (18-19) used this approach as a means for experimentally determining the undisturbed extracellular concentration, C_e^{∞}, and the absolute value of the slope, which they defined to be the "dialysis recovery". The term "recovery" is more usually employed to refer to the ratio, C_d^{out}/C_e^{∞}, under the restricted condition of $C_d^{in}=0$, which applies to the data in Figure 3. Eq. (4) suggests the use of the dialysate extraction fraction, $E_d=(C_d^{out}-C_d^{in})/(C_e^{\infty}-C_d^{in})$, as a generalized recovery when C_d^{in} is non-zero, as we have done for the curves in Figure 3. Lönnroth et al. observed that "recovery" was linear in C_d^{in} for adenosine (19), but nonlinear at low values of C_d^{in} for glucose (18).

Although the scheme of Lönnroth et al. can be used as a check on linearity of tissue behavior, dialysate measurements are less than conclusive tests of detailed kinetic tissue models of the type constructed in the Appendix. More sensitive tests would be provided by the measurement of tissue concentration profiles for comparison with theoretical simulations, such as those of Figure 4. Techniques are available for concentration profile measurement, e.g., electrochemical probes (7) or autoradiography with radioisotope-labeled substances.

At most flow rates a large difference in extraction fraction (recovery) is predicted between the quiescent and well-stirred external media cases (Figure 3). From this it is clear that results obtained with a "calibration" bath (15) can be misleading when the degree of convective mixing around the probe is uncharacterized. Some investigators have employed a gelled external medium to avoid convection (7). Even in the absence of convection, the gel will generally yield different extraction fractions than tissue. This is due, in part, to differences in volume fraction, hindrance and tortuosity factors between the gel and tissue (7). In addition, according to text Eqs.(9-10), microvascular exchange and tissue metabolism play an important role in tissue resistance, R_e, through their effect on the value of Γ. Hence, even a quiescent "calibration" bath has only limited relevance to *in vivo* probe performance in the absence of a quantitative theory taking all of these factors in account.

Figure 3 does demonstrate that the difference between *in vivo* and *in vitro* characteristics disappears at dialysate flow rates sufficiently low that the dialysate can nearly equilibrate with the tissue. Microdialysis at low flow rates would probably not be suitable for many kinetics experiments because of long dialysate collection times. On the other hand, near-equilibrium, low flow rate microdialysis might have attractive applications, such as in experiments with chronically implanted probes.

Although plotting E_d against Q_d, as in Figure 3, has some usefulness, the same information can be presented in a manner that is more amenable to further analysis. Data satisfying Eq.(4), when plotted as $-\ell n[1-E_d]$ against $1/Q_d$, yield straight lines. The slope from such a plot permits direct calculation of the product, PS, defined in Eq.(5).

The series resistance model of text Eqs.(2) and (4) could be extended to describe the change in behavior resulting from the formation of an abnormal layered structure surrounding the probe. Examples might include an edematous layer arising from the trauma of probe insertion, or gliosis following chronic implantation. Reduced microdialysis extraction is often ascribed to alterations in the probe membrane. The model offers possible alternative explanations based on properties of the abnormal layer(s), such as extracellular diffusion coefficient and volume fraction, extracellular and intracellular metabolism, and altered microvascular exchange.

The tissue mass transport resistance expression, Eq.(9), was derived using metabolism and exchange models that are linear or zero order in concentration. It is not expected that this expression will be quantitatively applicable to all chemical species of interest in microdialysis. What is important at this stage of microdialysis development is that Eq.(9) does contain descriptions for metabolism and exchange and demonstrates the importance of these processes. In addition, our treatment separates the contributions of the tissue, membrane and dialysate. Hence, the present analysis is at least qualitatively more useful than existing microdialysis theory lacking these factors (7). Furthermore, the concept of series and parallel mass transport resistances is general and applicable to probes of other geometry (6). As a result, this work has implications at various levels for much of the microdialysis currently performed.

Acknowledgment

The authors wish to acknowledge the helpful comments and suggestions of J.K. Hsiao, I.N. Mefford, K.H. Dykstra and those who reviewed the manuscript for Life Sciences.

Appendix

The variation in the radial (r) and axial (z) direction (Figures 1 and 2) of the species concentration, or activity, within the accessible volume fraction (ϕ_m) of the membrane is $C_m[r,z]$, $r_\beta<r<r_o$ and $0<z<L$. Likewise, the dialysate concentration in the annulus between the membrane and the inner cannula is $C_d[r,z]$, $r_\alpha<r<r_\beta$, the concentration in the extracellular fluid (ECF) volume fraction (ϕ_e) is $C_e[r,z]$, $r>r_o$, and the concentration in the cellular volume fraction (ϕ_i) is $C_i[r,z]$, $r>r_o$ for $0<z<L$. For equilibrium across the interfaces, $C_d[r_\beta,z]=C_m[r_\beta,z]$ and $C_m[r_o,z]=C_e[r_o,z]$. Far from the probe the extracellular fluid concentration approaches a uniform level $C_e[r\to\infty,z]=C_e^\infty$. For continuity of species mass flow rate, q, across the inner and outer membrane interfaces,

$$\frac{q}{2\pi r_\beta L} = \frac{\vartheta D_d(C_m - \overline{C}_d)}{(r_\beta - r_\alpha)} = D_m\phi_m\left(\frac{\partial C_m}{\partial r}\right) \quad \text{at} \quad r = r_\beta\,, \tag{A1}$$

and

$$\frac{q}{2\pi r_o L} = D_m\phi_m\left(\frac{\partial C_m}{\partial r}\right) = D_e\phi_e\left(\frac{\partial C_m}{\partial r}\right) \quad \text{at} \quad r = r_o\,. \tag{A2}$$

In the above D_d, D_m and D_e are the diffusion coefficients in the dialysate, membrane void fraction and ECF, respectively, and the dialysate concentration has been flow-averaged across the annulus according to the definition in the Nomenclature section. The product ϑD_d expresses the effective diffusion coefficient for the dialysate when the axial convective transport effects are taken into account. For negligible diffusion in the axial direction, mass balances on differential volumes within ϕ_m and ϕ_e are

$$\frac{\partial C_m}{\partial t} = \frac{1}{r}\frac{\partial}{\partial r}\left(rD_m\frac{\partial C_m}{\partial r}\right) = 0, \tag{A3}$$

and

$$\frac{\partial C_e}{\partial t} = \frac{1}{r}\frac{\partial}{\partial r}\left(rD_e\frac{\partial C_e}{\partial r}\right) - k_e^r C_e + k_{ie}^x C_i - k_{ei}^x C_e + k_{pe}^x C_{pA} - k_{ep}^x C_e = 0, \tag{A4}$$

in which k_{ie}^x and k_{ei}^x are the efflux and uptake rate constants for extracellular-to-intracellular exchange, k_{ep}^x and k_{pe}^x are the ECF-to-plasma efflux and uptake rate constants, k_e^r is the rate constant for irreversible extracellular metabolism, and C_{pA} is the unbound arterial plasma concentration. A useful relationship for ECF uptake is (9,12)

$$k_{pe}^x = \left(\frac{Q_b\phi_b}{\phi_e}\right)E_p, \tag{A5}$$

where ϕ_b is a fractional measure of the distribution volume of the substance in blood, Q_b is the microvascular blood flow rate per unit volume of tissue, and E_p is the plasma extraction fraction in the microvasculature analogous to E_d defined in text Eqs.(4)-(5)

$$E_p = \frac{C_{pA} - C_{pV}^{\infty}}{C_{pA} - C_e^{\infty}} = 1 - \exp\left[-\frac{p_{pe}s}{Q_b\phi_b}\right]. \tag{A6}$$

In the above, $p_{pe}s$, is the product of the plasma-ECF microvascular permeability (p_{pe}) multiplied by the microvascular exchange surface area per unit volume of tissue (s), and C_{pV} is the unbound venous plasma concentration. The ECF efflux rate constant, k_{ep}^x, and microvascular permeability, p_{ep}, are related to their uptake counterparts by $k_{ep}^x/p_{ep} = k_{pe}^x/p_{pe}$.

Under the assumption that the transcellular pathway can be neglected in comparison with ECF diffusion, a chemical species mass balance on the cellular compartment can be written as

$$\phi_i\left(\frac{\partial C_i}{\partial t}\right) = \phi_e(k_{ei}^x C_e - k_{ie}^x C_i) + \phi_i(G_i - k_i^r C_i) = 0, \tag{A7}$$

in which intracellular species metabolism has been incorporated as a constant rate of species generation, G_i, and an irreversible first order degradation with rate constant, k_i^r. Eq.(A4), in combination with Eq.(A7), reduces to the following predictive relationship for the undisturbed ECF concentration far from the probe in steady-state

$$C_e^{\infty} = \left(\frac{k_{pe}^x}{k_{ep}^x + k_e^r + k_c^r}\right)C_{pA} + \frac{\phi_i k_{ie}^x G_i}{\left(k_{ep}^x + k_e^r + k_c^r\right)\left(\phi_e k_{ie}^x + \phi_i k_i^r\right)}. \tag{A8}$$

For steady-state with constant diffusion and rate coefficients Eqs.(A4), (A7) and (A8) yield

$$\frac{r_o}{r}\frac{\partial}{\partial(r/r_o)}\left[\frac{r}{r_o}\frac{\partial(C_e - C_e^{\infty})}{\partial(r/r_o)}\right] - \left(\frac{r_o}{\Gamma}\right)^2\left(C_e - C_e^{\infty}\right) = 0, \tag{A9}$$

where Γ is a characteristic tissue length scale for combined diffusion, reaction and permeation given by text Eq.(10), in which k_c^r is a composite rate constant for intracellular degradation

$$k_c^r = \frac{\phi_i k_{ei}^x k_i^r}{\phi_e k_{ie}^x + \phi_i k_i^r}. \tag{A10}$$

Eqs.(A1)-(A3) and (A9) can be solved to yield expressions for the concentration profiles within the membrane and the ECF. Substitution of the profiles and the first relation for q from Eq.(A1) into text Eq.(1) yields text Eqs.(7)-(9) for R_d, R_m and R_e, which can in turn be used to simplify the profile expressions to

$$\frac{C_m[r,z]-C_e^\infty}{\bar{C}_d[z]-C_e^\infty} = \frac{\left(\frac{\ell n(r/r_o)}{\ell n(r_\beta/r_o)}\right)R_m + R_e}{R_d+R_m+R_e}, \tag{A11}$$

and,

$$\frac{C_e[r,z]-C_e^\infty}{\bar{C}_d[z]-C_e^\infty} = \frac{\left(\frac{K_0[r/\Gamma]}{K_0[r_o/\Gamma]}\right)R_e}{R_d+R_m+R_e}. \tag{A12}$$

The axial dialysate profile, $\bar{C}_d[z]$, is obtained by integration of text Eqs.(2) and (3)

$$\frac{\bar{C}_d[z]-\bar{C}_d[0]}{C_e^\infty-\bar{C}_d[0]} = 1-\exp\left[-\frac{z/L}{Q_d(R_d+R_m+R_e)}\right]. \tag{A13}$$

Quiescent Medium: In a quiescent, inert medium the rate constants in text Eq.(10) vanish, the value for the parameter Γ becomes infinite, $K_0[r_o/\Gamma]$ becomes zero, and Eq.(A12) cannot be employed for describing the external medium concentration profile. It would be desirable to reformulate Eq.(A9) to include diffusion in the z direction. The solution to the resulting equations would describe the deviations from Eq.(A12) in the regions around the two ends of the probe membrane. In the absence of such a description we take the simpler, but approximate, approach of representing the probe by a sphere of radius ϖ_o possessing the same area, S_q, as the outer membrane surface, that is,

$$S_q = 4\pi\varpi_o^2 = 2\pi r_o L. \tag{A14}$$

The profile is then found by solution in spherical coordinates of

$$\frac{d}{d\varpi}\left(\varpi^2 D_q \frac{dC_q}{d\varpi}\right) = 0, \tag{A15}$$

which yields for the mass flow rate across S_q

$$q = D_q\phi_q S_q\left(\frac{dC_q}{d\varpi}\right)_{\varpi=\varpi_o} = D_q\phi_q S_q\left(\frac{C_q^\infty - C_o}{\varpi_o}\right). \tag{A16}$$

The comparison of Eq.(A16) with text Eqs.(1) and (6), together with Eq.(A14), leads to text Eq.(11).

Nomenclature

C	concentration or activity, various units
D	diffusion coefficient, length^2/time
E	extraction fraction, dimensionless
G	species generation rate, mass/(length^3·time)
H	fractional reduction in diffusivity owing to hindrance effects, dimensionless
K_n	modified Bessel function of the second kind of order n
k	rate constant, time^{-1}
L	accessible length of membrane, length
P	permeability, length/time
p	microvascular permeability, length/time
Q	volumetric flow rate, length^3/time
q	mass flow rate, mass/time
R	mass transport resistance, time/length^3
r	radial distance from probe axis, length
S	surface area, length^2
s	microvascular exchange surface area per unit volume of tissue, length^2/length^3
T	characteristic time
t	time
z	distance along probe axis from inlet end of membrane, length
ϑ	coefficient expressing effect of dialysate flow in the axial direction on exchange between membrane and dialysate, dimensionless
Γ	extracellular concentration profile penetration depth parameter, length
λ	increase in diffusional path length due to tortuosity, dimensionless
ϕ	volume fraction or fractional distribution volume, dimensionless
ϖ	spherical radial coordinate

Subscripts and superscripts

A	arterial
b	blood
c	composite effect of intracellular metabolism and extracellular-intracellular exchange, Appendix Eq.(A10)
D	pertaining to radial diffusion in the dialysate annulus
d	dialysate
e	extracellular phase
eff	effective value
ext	medium contiguous to the external surface of probe membrane
i	intracellular phase
in	dialysate inlet
m	phase of dialysis membrane through which transport occurs
o	outer surface of probe membrane
out	dialysate outlet
p	blood plasma
Q	pertaining to axial convection in the dialysate annulus
q	quiescent medium (no convective mixing)
r	metabolism
s	well-stirred medium (complete convective mixing)
x	exchange between phases
∞	value far from the probe; undisturbed value

Overbar

Denotes flow-averaging defined as follows for the dialysate concentration in the concentric annulus between the inner cannula and the probe membrane

$$\bar{C}_d[z] = \left(\int_{r_\alpha}^{r_\beta} 2\pi r C_d[r,z]v[r]dr\right) / \left(\int_{r_\alpha}^{r_\beta} 2\pi r v[r]dr\right) = \left(\int_{r_\alpha}^{r_\beta} 2\pi r C_d[r,z]v[r]dr\right) / Q_d \, .$$

The local dialysate velocity, v, varies with radial position and is assumed to be everywhere parallel to the probe axis (Figure 2).

References

1. Bibliography of Microdialysis, Bioanalytical Systems, Inc, West Lafayette, Indiana, 1986, revised Dec. 1988.
2. H. BENVENISTE, J. Neurochem. 52 1667-1679 (1989).
3. J.M.R. DELGADO, F.V. DEFEUDIS, R.H. ROTH, D.K. RYUGO, and B.M. MITRUKA, Arch. int. Pharmacodyn. 198 9-21 (1972).
4. L. BITO, H. DAVSON, E. LEVIN, M. MURRAY, and N. SNIDER, J. Neurochem. 13 1057-1067 (1966).
5. P.F. MORRISON, P.M. BUNGAY, and R.L. DEDRICK, Abstract from the International Symposium on Microdialysis, Indianapolis, May 18-19, 1989, published in Current Separations 9 75 (May 1989).
6. I. JACOBSON, M. SANDBERG, and A. HAMBERGER, J. Neurosci. Meth. 15 263-268 (1985).
7. H. BENVENISTE, A.J. HANSEN, and N.S. OTTOSEN, J. Neurochem. 52 1741-1750 (1989).
8. E. KLEIN, F.F. HOLLAND, A. DONNAUD, A. LEBEOUF, and K. EBERLE, J. Membrane Sci. 2 349-364 (1977).
9. J.D. FENSTERMACHER, and S.I. RAPOPORT, Handbook of Physiology - The Cardiovascular System, Vol. 4, Chap. 21, pp. 969-1000, American Physiological Society Bethesda, Maryland (1984).
10. R.B. BIRD, W.E. STEWART, and E.N. LIGHTFOOT, Transport Phenomena, p. 404, John Wiley & Sons, New York (1960).
11. E. KLEIN, F.F. HOLLAND, and K. EBERLE, J. Membrane Sci. 5 173-188 (1979).
12. C.S. PATLAK, and J.D. FENSTERMACHER, Am. J. Physiol. 229 877-884 (1975).
13. M. ABRAMOWITZ, and I.A. STEGUN (Eds.), Handbook of Mathematical Functions, National Bureau of Standards, Washington D.C., 1964, or Dover Publications, New York, 1965.
14. M.E. RICE, G.A. GERHARDT, P.M. HIERL, G. NAGY, and R.N. ADAMS, Neurosci. 15 891-902 (1985).
15. G.M. ALEXANDER, J.R. GROTHUSEN, and R.J. SCHWARTZMAN, Life Sci. 43 595-601 (1988).
16. R. MILLS, J. Phys. Chem. 77 685-688 (1973).
17. J. DEDEK, R. BAUMES, N. TIEN-DUC, R. GOMENI, and J. KORF, J. Neurochem. 33 687-695 (1979).
18. P. LÖNNROTH, P.A. JANSSON, and U. SMITH, Am. J. Physiol. 253 (Endocrinol. Metab. 16) E228-E231 (1987).
19. P. LÖNNROTH, P.A. JANSSON, B.B. FREDHOLM, and U. SMITH, Am. J. Physiol. 256 (Endocrinol. Metab. 16) E250-E255 (1989).